NUMERICAL MODELLING OF IMPACTS INTO ASTEROID (16) PSYCHE ANALOGUES

S. D. Raducan[1], T. M. Davison[1], G. S. Collins[1]. [1]Impacts and Astromaterials Research Centre, Department of Earth Science and Engineering, Imperial College London, London, SW7 2AZ, United Kingdom (E-mail: s.raducan16@imperial.ac.uk).

Introduction: M-type asteroids are widely believed to be the exposed cores of differentiated planetesimals [1]. Observations of asteroid (16) Psyche, the most massive M-type asteroid in the main belt [1], revealed an unusually high radar albedo which is consistent with iron-nickel meteorites observed in the laboratory [2] and a much larger thermal inertia than that observed in other asteroids [3]. In addition to the high density estimates, in the 3.8–4.6 g/cm^3 range [2, 4, 5], these observations represent compelling evidence for a metal-rich surface.

The asteroid will be visited by the Discovery-class mission 'Psyche' [6, 7], which will be launched in 2022 and arrive at Psyche in 2026, after 21 months in orbit. The mission will determine: whether Psyche is comprised of highly reduced material that never melted [6] or whether it is an exposed metal core of a protoplanet; the relative ages of surface materials; and the topography of the asteroid.

One hypothesis to explain Psyche's metal composition supposes that most of the primitive crust and mantle of the differentiated progenitor asteroid was stripped off by hit-and-run collisions, leaving behind a bare core [8]. However, according to recent modelling, hit-and-run collisions are not able to strip off the entirety of the mantle, without disrupting the core. It has been proposed that the remaining silicate fragments were removed by subsequent smaller collisions and micrometeorite impacts [9], producing a regolith layer of metal intermixed with a small fraction of silicates.

Here we present simulations of impacts on Psyche after hit-and-run collisions stripped the bulk of its mantle. We explore the size and morphology of craters resulting from different impact scenarios, and quantify the efficiency of small impacts in eroding residual silicate mantles of different thicknesses on a post hit-and-run Psyche.

Numerical Methods: We used the iSALE 2D shock physics code [10, 11] to simulate impacts into post hit-and-run Psyche. We considered three different scenarios:

a) Impacts into an intact iron core covered by a thin layer of silicate regolith. This was the main impact scenario modelled and it assumed that Psyche started as a Vesta-like body [12, 13], that then experienced several hit-and-run collisions, which stripped off most of the mantle material. Our impact simulations of subsequent impacts were performed into a two-layer target, where the mantle was only several tens of km. The upper layer, the mantle, was modelled using the ANEOS [14] EOS for dunite [15] and a strength model typical for rock materials, in which strength is reduced with strain as damage accumulates [10]. The lower layer, the iron core, was modelled using the ANEOS EOS for iron and the Johnson-Cook strength model [16]. The thickness of the mantle to the impactor radius ratio, h/a, was varied between 0.5 and 8.

b) Impacts into non-porous intact iron targets. To understand the morphology and size of a crater formed into an exposed core, this impact scenario considered that the entirety of the silicate mantle was removed by hit-and-run collisions and subsequent impacts. Therefore, the impact simulations were performed into a non-porous iron target.

c) Impacts into a shattered iron target, with 40% porosity. This impact scenario follows the same rationale as in b), but in this case the hit-and-run collisions shattered the core, leaving behind a rubble pile. The target was modelled using the Johnson-Cook strength and damage models for Armco iron [17].

In all simulations, the impactor was modelled as a 10 km diameter dunite sphere, at 5 and 10 km/s. Tracer particles were placed across the high-resolution domain and their mass and velocity were recorded if they crossed a fixed altitude, equal to one impactor diameter. Tracers that crossed this line were identified as ejecta in post-processing if their maximum speed exceeded the escape velocity of the target.

Crater size: In scenario a), the impactor's kinetic energy is dissipated into the dunite mantle layer, causing a shallower crater to be formed in the core (Fig. 1a), compared to the non-layered scenario b), where the 10 km dunite sphere at 5 km/s produced a simple bowl shaped crater, with a diameter of $\approx$ 40 km (Fig. 1b). For the same impact conditions, an impact into a damaged, porous iron core (Fig. 1c) results in a slightly wider, $\approx$ 50 km diameter, but much deeper crater.

Ejected mass: We investigated the ejected mass from a 10 km dunite sphere impacting a two-layer Psyche target, at 5 and 10 km/s (scenario a)). Figure 2 shows ejected mantle mass and total ejected mass, as a function of the upper layer thickness, normalised by the impactor radius, h/a. The ejected mass for each simulation is normalised by the amount of ejected mass from an equivalent impact into a half-space mantle target, with no lower layer.

For very thin mantle layers, the ejected material originated from both the mantle and the core, and its total mass was lower than in the homogeneous mantle case. On the

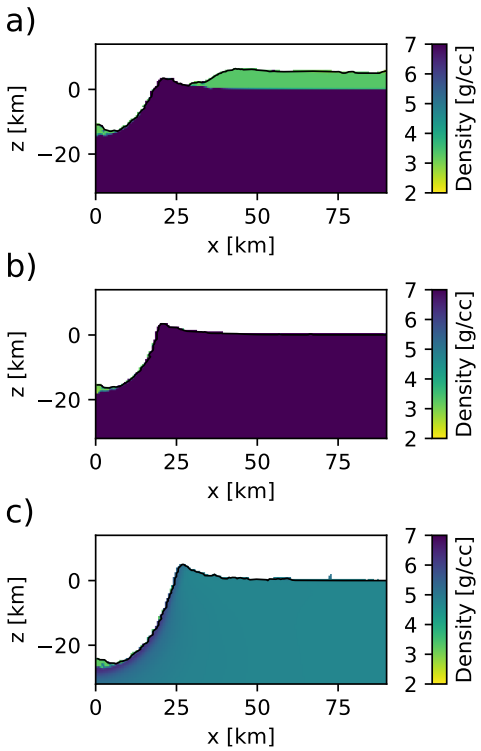

Figure 1: Crater morphologies for impacts into three different Psyche target scenarios: a) intact iron core with a dunite mantle, b) intact iron core, and c) porous (40%) damaged iron core.

other hand, impacts into mantle layers with $1 < h/a < 3$ ejected up to 60% more mantle mass than in the homogeneous mantle case. Due to the difference in the mechanical impedance (the product of density and wave speed) between the upper and lower layers, the shock wave reflects at the boundary, being only partially transmitted into the substrate. As a result, more energy is retained in the shallow subsurface, which amplifies ejection speeds in the upper layer. For impacts into mantle layers with $h/a > 5$, the influence of the core on the excavation flow is no longer significant and the total ejected mass converges to the mass ejected in the homogeneous mantle case.

We found that there is clearly an amplification in the amount of ejected mantle mass in thin-mantle impact scenarios, compared to impacts into thick mantles, caused by the proximity of the iron core to the surface. However, despite this amplification, ejection of mantle material from inside the crater does not appear to be sufficient to erode a residual mantle with a thickness of several km or more. Based on models of Pysche's expected impact flux, the best-case scenario predicts that only a few km of mantle could have eroded been by small impacts (<20 km diameter). This suggests that either hit-and-run collisions were

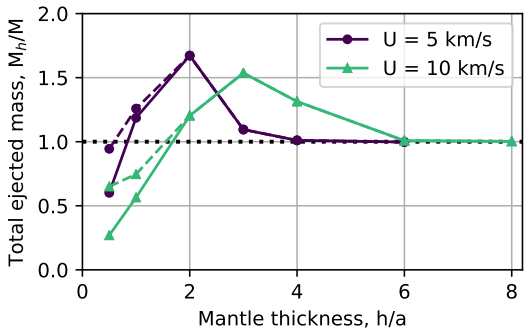

Figure 2: Total ejected target mass (dashed line) and total ejected mantle mass (solid line) from scenario a) impacts, normalised by the amount of mass ejected in a dunite half-space impact simulation, as a function of normalised mantle thickness.

more efficient at eroding the mantle than anticipated, or that other mechanisms are responsible for removing the residual mantle. One potential mechanism currently under investigation is impact-induced spallation of mantle on the opposite side of Psyche to the impact, in high-energy sub-catastrophic disruption collisions.

Conclusions: Numerical simulations of impacts into analogue Psyche targets suggest that in a two-layer mantle-core scenario, close proximity of the core to the surface would enable impacts to be up to 60% more efficient at removing silicate mantle covering the core. However, mantle stripping by impacts via crater ejecta is only capable of eroding a few km of mantle on Psyche.

Acknowledgements: We gratefully acknowledge the developers of iSALE (www.isale-code.de) and STFC for funding (Grant ST/N000803/1).

References: [1] Tholen, D. J. (1984) *Ph.D. Thesis*, [2] Shepard, M. K. et al. (2017) *Icarus*, 281:388–403. [3] Matter, A. et al. (2013) *Icarus*, 226:419–427. [4] Hanuš, J. et al. (2017) *A&A*, 601:A114. [5] Drummond, J. D. et al. (2018) *Icarus*, 305:174–185. [6] Elkins-Tanton, L. et al. (2016) *LPSC 47*,1631. [7] Elkins-Tanton, L. et al. (2017) *LPSC 48*,1718. [8] Asphaug, E. et al. (2006) *Nature*, 439:155–160. [9] Sanchez, J. A. et al. (2017) *AJ*, 153:29. [10] Collins, G. S. et al. (2004) *Meteorit. Planet. Sci*, 39:217–231. [11] Wünnemann, K. et al. (2006) *Icarus*, 180:514–527. [12] Ivanov, B. A. et al. (2010) *Geol. Soc. Spec. Pap.* 465:29–49. [13] Ivanov, B. A. & Melosh, H. J. (2013) *J. Geophys. Res: Planets*, 118:1545–1557. [14] Thompson, S. L. & Lauson, H. S. (1974) tech. rep. SC-RR–71-0714 Sandia Labs. [15] Benz, W. et al. (1989) *Icarus*, 81:113–131. [16] Johnson, G. R. & Cook, W. H. (1983) *Proc. 7th International Symposium on Ballistics*,541–547. [17] Johnson, G. R. & Cook, W. H. (1985) *Eng Fract Mech*, 21:31–48.